COMPUTATIONAL CONTINUUM MECHANICS

ВЫЧИСЛИТЕЛЬНАЯ МЕХАНИКА СЛОШНЫХ СРЕД

Computational Continuum Mechanics. 2021. Vol. 14. No. 2. pp. 233-244 DOI: 10.7242/1999-6691/2021.14.2.20

INFLUENCE OF A VARIABLE THERMAL DIFFUSION COEFFICIENT ON CONVECTION OF A BINARY MIXTURE IN RECTANGULAR CAVITIES

T.P. Lyubimova[1,2], K.S. Rushinskaya[1] and N.A. Zubova[1]

[1]*Institute of Continuous Media Mechanics UB RAS, Perm, Russian Federation*
[2]*Perm National Research State University, Perm, Russian Federation*

The paper presents the results of numerical simulation of non-linear convection regimes of a NaCl aqueous solution in square and horizontally elongated rectangular cavities with hard and impermeable boundaries. The vertical boundaries of the cavities are thermally insulated, and the horizontal ones are maintained at different constant temperatures, which corresponds to heating from below. Calculations are carried out within the non-stationary approach using of Boussinesq approximation and taking into account the polynomial temperature dependence of the thermal diffusion coefficient. According to this approximation, at K, the thermal diffusion coefficient changes sign, and thus the direction of the concentration gradient, also changes. The temperature gradients on the horizontal boundaries are chosen so that the thermal diffusion coefficient changes sign inside the cavity. Other transport coefficients are considered to be constant. Simulations were performed for the cases of the action of the Earth gravity and at reduced gravity conditions. Earth-gravity and reduced-gravity conditions. Based on the results of simulations, the local and integral characteristics of non-linear regimes were obtained, and the structure of the emerging flow and the distribution of NaCl concentration were determined. It is shown that the temperature dependence of the thermal diffusion coefficient only slightly affect the structure and intensity of the emerging flow but significantly reduces the degree of separation of mixture components. Under the gravitational field of the Earth, an oscillatory four-vortex flow with reconnection of vortices occurs in the square cavity, and a multi-vortex flow - in the rectangular cavity. The characteristics of the multi-vortex flow vary irregularly. At reduced gravity, a stationary flow is observed in both square and rectangular cavities. Under microgravity conditions, the concentration isolines are “frozen” into the stream function field, i.e., the similarity between the fields is pronounced.

Key words: convection, binary mixture, diffusion, thermal diffusion, thermal diffusion coefficient

1. Introduction

Investigations of heat and mass transfer in multicomponent mixtures with allowance for diffusion and thermal diffusion have a wide range of applications. Examples would be hydrocarbon production [1], filtration of pollutants [2–4], their distribution [5–8], recovery of geothermal energy [9]. A similar approach is applicable to modeling complex biological fluids, colloidal suspensions and metals [10–14].

To take into account the effects of diffusion and thermal diffusion, it is necessary to know the values of the transfer coefficients. There are many works devoted to the determination of the transfer coefficients in specific multicomponent mixtures under various fixed external conditions (values of temperature, pressure) and different ratios of the mass fractions of the mixture components [15–19]. In a number of works, the diffusion and thermal diffusion (Soret) coefficients are found as functions of the temperature and concentration of the mixture components [15, 20–27]. Analysis of literature data shows that binary organic liquid mixtures can be divided into three groups by the nature of the dependence of the Soret coefficient on temperature and concentration. The first group demonstrates a non-monotonic relationship between the Soret coefficient and the concentration, where that relationship persists with increasing temperature and concentration does not change with increasing temperature [25, 26]. The second group is also characterized by a non-monotonic decrease in the modulus of the Soret coefficient with increasing temperature, and the concentration value at which the sign of the Soret coefficient changes does not depend on temperature [27]. Mixtures of the third group have a temperature invariant point, at which the temperature does not affect the Soret coefficient, which is not equal to zero [15, 26].

Usually, when simulating convective phenomena in mixtures, it is assumed that the deviations of temperature and concentration from the average (or initial) values are small; therefore, the temperature and concentration changes in the transport coefficients are not taken into account [28–30]. However, in the case of sufficiently large temperature and concentration gradients, the variability of the coefficients can significantly affect the behavior of the mixture. In [31], the influence of the temperature and concentration

Email addresses for correspondence: lyubimovat@mail.ru

conditionality of the Soret coefficient on the distribution of the solute of a binary mixture in the absence of natural convection is analyzed.

In this work, we investigate the onset and non-linear regimes of convection of an aqueous NaCl solution in a horizontal rectangular cavity when heated from below. The temperature difference between the lower and upper boundaries is 40 degrees. Modeling is carried out taking into account the polynomial dependence of the thermal diffusion coefficient on temperature [21, 31], a feature of which is that the thermal diffusion coefficient changes sign at a certain temperature value. In this work, such a temperature range has been chosen for discussion that the sign of the thermal diffusion coefficient changes inside the cavity. Other transport coefficient factors are considered constant.

2. Problem statement and solution method

The thermal concentration convection of a binary mixture in square and horizontally elongated rectangular cavities heated from below is considered. (Fig. 1). The density of the mixture ρ is considered as linearly dependent on the temperature T and the solute concentration C:

$$\rho = \rho_0\left(1-\beta_T\left(T-T_0\right)-\beta_C\left(C-C_0\right)\right). \tag{1}$$

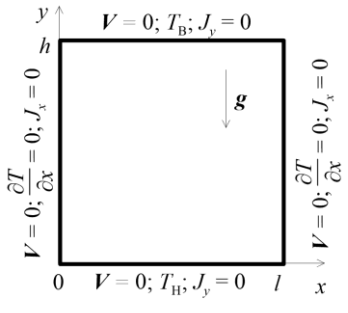

Fig. 1. Geometry and boundary conditions of the problem.

Here $\beta_T = \left(-1/\rho_0\right)\left(\partial\rho/\partial T\right)\big|_C$ and $\beta_C = \left(-1/\rho_0\right)\left(\partial\rho/\partial C\right)\big|_T$ are the coefficients of thermal and concentration expansion, respectively; ρ_0, C_0 and T_0 are the average values of density, solute concentration and temperature of mixture.

The effects of barodiffusion and diffusion thermal conductivity are neglected. The coefficients of viscosity ν, molecular diffusion D, and thermal diffusion χ are assumed to be constant, and the thermal diffusion coefficient D_T is assumed to depend on temperature according to a polynomial law in accordance with [21, 31].

Given these assumptions into account, the nonstationary equations of thermal concentration convection of a binary mixture in the Boussinesq approximation have this form:

$$\partial_t \boldsymbol{V} + \left(\boldsymbol{V}\cdot\nabla\right)\boldsymbol{V} = -\rho_0^{-1}\nabla p + \nu\nabla^2\boldsymbol{V} + \left[1-\beta_T\left(T-T_0\right)-\beta_C\left(C-C_0\right)\right]\boldsymbol{g}, \tag{2}$$

$$\partial_t T + \left(\boldsymbol{V}\cdot\nabla\right)T = \chi\Delta T, \tag{3}$$

$$\partial_t C + \left(\boldsymbol{V}\cdot\nabla\right)C = D\Delta C + D_T\left(T\right)\Delta T, \tag{4}$$

$$\nabla\cdot\boldsymbol{V} = 0. \tag{5}$$

Here $\boldsymbol{V}$ is the velocity vector; p is the pressure; $\boldsymbol{g}$ is the vector of gravity acceleration; symbol ∂_t denotes time t derivative; ∇ is the nabla operator; Δ is the two-dimensional Laplacian.

The boundaries of the cavity are considered rigid, impermeable to the substance. Their horizontal components are maintained at constant but different temperatures, corresponding to heating from below, while the lateral components are thermally insulated. The boundary conditions for the concentration are that the diffusion flux of the substance J is equal to zero (Fig. 1):

$$x = 0; l: \quad \boldsymbol{V} = 0, \quad \frac{\partial T}{\partial x} = 0, \quad J_x = -\rho_0 D\frac{\partial C}{\partial x} + D_T\left(T\right)\frac{\partial T}{\partial x} = 0, \tag{6}$$

$$y = 0: \quad \boldsymbol{V} = 0, \quad T = T_{\mathrm{L}}, \quad J_y = -\rho_0 D\frac{\partial C}{\partial y} + D_T\left(T\right)\frac{\partial T}{\partial y} = 0, \tag{7}$$

$$y = h: \quad \boldsymbol{V} = 0, \quad T = T_{\mathrm{U}}, \quad J_y = -\rho_0 D\frac{\partial C}{\partial y} + D_T\left(T\right)\frac{\partial T}{\partial y} = 0. \tag{8}$$

A square cavity with a side of 0.01 m and a rectangular cavity with a length of $l = 0{,}05$ m and height of $h = 0{,}01$ m were considered. The temperature was taken equal to $T_{\mathrm{L}} = 318$ K at the lower boundary and

$T_U = 278$ K at the upper boundary. The calculations are performed for the following values of the gravity acceleration g: $g = g_0$, which corresponds to the Earth conditions, as well as for $g = g_0 \cdot 10^{-1}$ and $g = g_0 \cdot 10^{-2}$, that is, in reduced gravity conditions.

The object of the study was an aqueous NaCl solution with a mass fraction of a dissolved substance $C_0 = 0,0285$ at an average temperature $T_0 = 298$ K. The thermal and physical parameters of this mixture are presented in the table and taken from [31–33].

Table. Thermal and physical parameters of an aqueous solution of NaCl

ρ_0, kg/m^3	ν, m^2/s	χ, m^2/s	β_T, K^{-1}	β_C	D, m^2/s
1050,0	$1{,}03\cdot10^{-6}$	$1{,}47\cdot10^{-7}$	$1{,}9\cdot10^{-4}$	-0,755	$1{,}512\cdot10^{-9}$

The thermal diffusion coefficient was considered to be temperature dependent according to the following law [21, 31]:

$$D_T(T) \approx 10^{-10}\left(1{,}463 - 0{,}00885T + 0{,}0000131T^2\right) \text{m}^2/(\text{s}\cdot\text{K}). \quad (9)$$

At temperature $T_0 = 298$ K, it was equal to $D_T \approx -1{,}58\cdot10^{-12}$ m^2/(s · K); at a temperature difference of 40 K, according to (9), inside the region the thermal diffusion coefficient changed sign; at temperature $T^* \approx 285{,}4$ K it varied from the upper boundary of the cavity to the lower one in the range from $-2{,}66\cdot10^{-11}$ to $2{,}33\cdot10^{-11}$ m^2/(s · K).

At the initial moment of time, it is assumed that the liquid is stationary, the solute concentration in the cavity is uniform, and the temperature linearly depends on the vertical coordinate.

The calculations were carried out in the ANSYS Fluent software package, which implements the finite volume method. A grid with square cells uniform in spatial variables was used, the grid step was $5\cdot10^{-5}$ m, and the time step was constant and equal to 1s. The selected sizes of the computational grid provided 5 nodes to resolve the concentration boundary layer. The equations were discretized using the second order of approximation in time and the third one in space.

3. Numerical results

Taking into account the polynomial form $D_T(T)$ (9) in that part of the cavity where the temperature is higher than $T^* \approx 285{,}4$ K, the thermal diffusion coefficient is negative. This means that, due to the effect of thermal diffusion, the heavy component of the mixture accumulates in the warmer zone of the cavity, and the light one diffuses into the colder zone. In the case of heating from below, a stable density stratification of the mixture is formed in the cavity. On the contrary, when heated from above, the dependence of density on temperature leads to an unstable density stratification. Then, as known from [34], at a certain value of the Rayleigh number, the mechanical equilibrium of the mixture becomes unstable, and convection is always excited in a monotonic manner.

In the upper part of the cavity, where the temperature is below $T^* \approx 285{,}4$ K and, according to (9), the thermal diffusion coefficient is positive, a stable density stratification, which does not cause convective flow, arises under the action of thermal diffusion. However, it can be expected that the flow from the lower part of the cavity will also penetrate into this region and, as a consequence, the mixture will separate, but it will be smaller in comparison with the case of a constant thermal diffusion coefficient.

3.1. Square cavity

3.1.1. The case of the action of the Earth gravity. We consider the effect of the Earth gravity on the mixture. In this case, the conditions specified in this work correspond to the Rayleigh number $\text{Ra} = g\beta_T\Delta T h^3/(\nu\chi) \approx 1{,}23\cdot10^5$, which significantly exceeds its critical value $\text{Ra}_c = 2{,}98\cdot10^3$ found at a constant thermal diffusion coefficient equal to $D_T \approx -1{,}58\cdot10^{-12}$ m^2/(s · K). In the ANSYS Fluent software

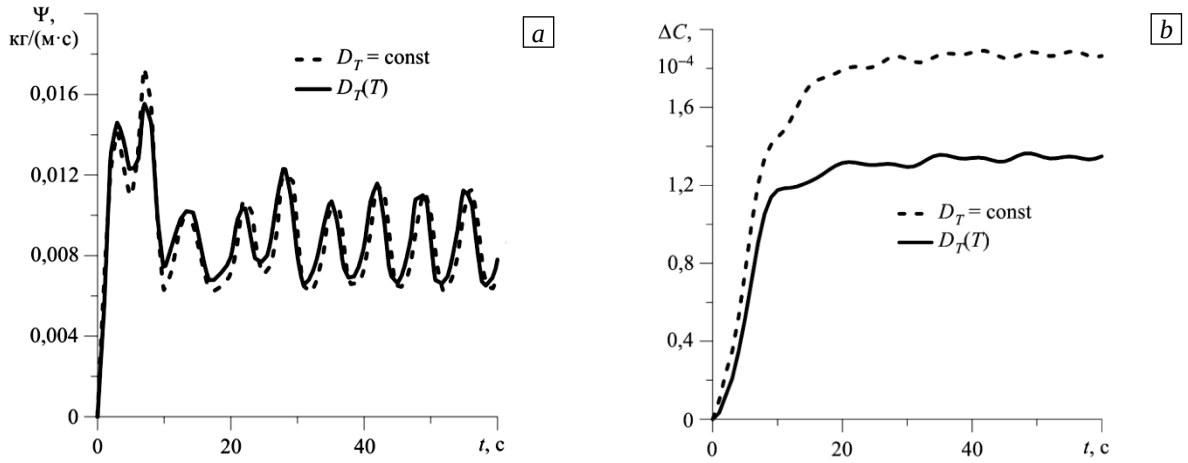

Fig. 2. Temporal evolution in the cavity of the maximum value of the stream function (*a*) and the concentration difference between the centers of the upper and lower boundaries (*b*) under the action of the Earth gravity.

package used for calculations, the stream function Ψ is introduced as $\rho u = \partial\Psi/\partial y$, $\rho v = -\partial\Psi/\partial x$, where u and v are the x- and y-components of the velocity vector.

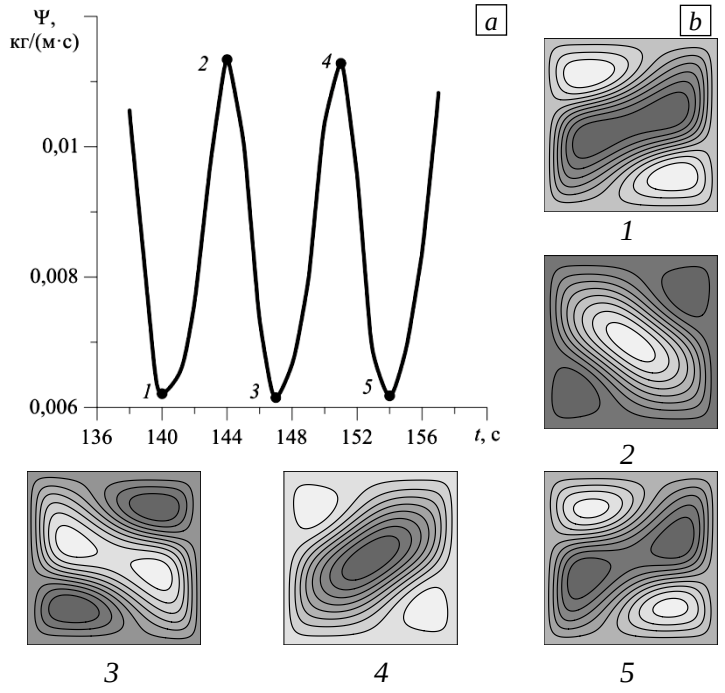

Fig. 3. Fragment of the temporal evolution of the maximum value of the stream function in the cavity (*a*) and the change in the field of the stream function during the oscillation period (*b*) under the influence of the Earth gravity.

Figure 2 shows data on the temporal evolution of the maximum value of the stream function in the cavity and the difference in solute concentrations between the centers of the upper and lower boundaries of the cavity, obtained at a constant value of the thermal diffusion coefficient (dashed lines) and when dependence (9) is taken into account (solid lines).

As can be seen, taking into account $D_T(T)$ as a function of temperature has little effect on the emergence of instability and the formation of the flow. The flow, both in the cases of a constant thermal diffusion coefficient and its dependence on temperature, arises very quickly (there is practically no non-convective period at short times), then a transition to an oscillatory regime takes place (Fig. 2*a*). When $D_T(T)$ is taken into account, only a slight increase in the flow intensity occurs. The effect of changing the direction of the concentration gradient inside the cavity on the separation of the mixture is more significant; it leads to the fact that the maximum separation of the mixture in the case of a variable thermal diffusion coefficient is lower than with its constant value, by about 1.4 times (Fig. 2*b*).

With the passage of time, a regime of stationary oscillations with vortex reconnection is established (Fig. 3), this regime is similar to that observed in [35] at a constant thermal diffusion coefficient. The concentration distribution in the cavity is uniform in its central part and varies greatly near the boundaries (Fig. 4*a*, *b*). In Fig. 4*b*, the dashed line shows the $T^* = 285,4$ K isotherm delimiting the regions in which the thermal diffusion coefficient has different signs. The region where $D_T(T)$ is positive is pressed against the upper boundary of the cavity due to the strong flow. The concentration profiles demonstrate strong, in comparison with flow at a constant D_T, changes near the horizontal boundaries of the cavity, also associated with a change in the sign of the thermal diffusion coefficient in the upper part of the cavity (Fig. 4*c*). Concentration gradients in areas below

and above the $T^* = 285,4$ K isotherm are directed towards it; maximum value of solute concentration along the line $x = 0,005$ m in the case of a temperature-dependent thermal diffusion coefficient is achieved precisely at the point of $D_T(T)$ sign change, while at a constant D_T the mixture concentration reaches maximum value at the upper boundary of the cavity.

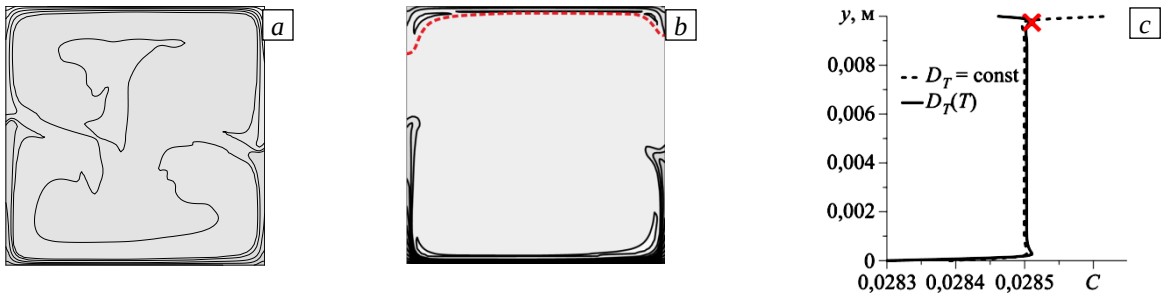

Fig. 4. Distribution of the solute concentration under the conditions of Earth gravity at time $t = 60$ s at a constant (*a*) and temperature-dependent (*b*) coefficient of thermal diffusion (dashed line shows isotherm $T^* = 285,4$ K, along which $D_T(T) \approx 0$ m^2/(s·K)); concentration profiles (*c*) along line $x = 0,005$ m (symbol X corresponds to the point where the thermal diffusion coefficient changes sign).

3.1.2. The gravitational force that is ten times less than that of the Earth. With a decrease in the magnitude of the gravitational force, convection occurs later: a sharp increase in the intensity of the flow is observed at $t \approx 50$ s (Fig. 5*a*). Subsequently, a stationary flow is formed in the cavity. Since there is a change in the sign of the thermal diffusion coefficient inside the cavity when taking into account that $D_T(T)$, the degree of maximum separation of the mixture in this case decreases in comparison with the degree at a constant value D_T by about 1,2 times (Fig. 5*b*). This is slightly lower than in the conditions of Earth gravity.

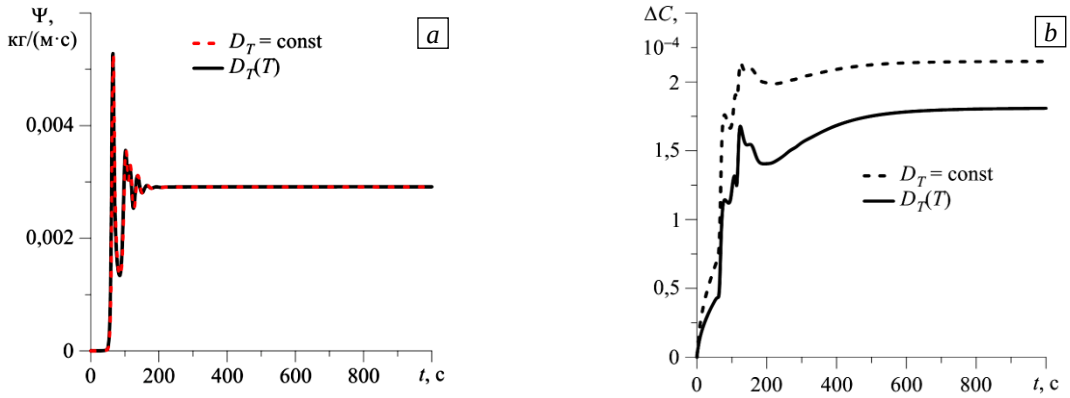

Fig. 5. Temporal evolution of the maximum value of the stream function in the cavity (*a*) and the concentration difference between the centers of the upper and lower boundaries (*b*) at a gravity ten times less than the Earth one.

The stationary flow, which arises under the gravitational force, which is ten times less than that of the Earth, has 2-vortex form both at a constant value of the thermal diffusion coefficient and at $D_T(T)$ (Fig. 6*a*). Since the Schmidt number is large ($\mathrm{Sc} = \nu/D = 681$), the concentration isolines are "frozen" in the flow field (that is, both fields have a pronounced similarity). There are two regions where the concentration is practically constant, and gradients are observed near the boundaries of the cavity and at the boundaries of the vortices (Fig. 6*b*).

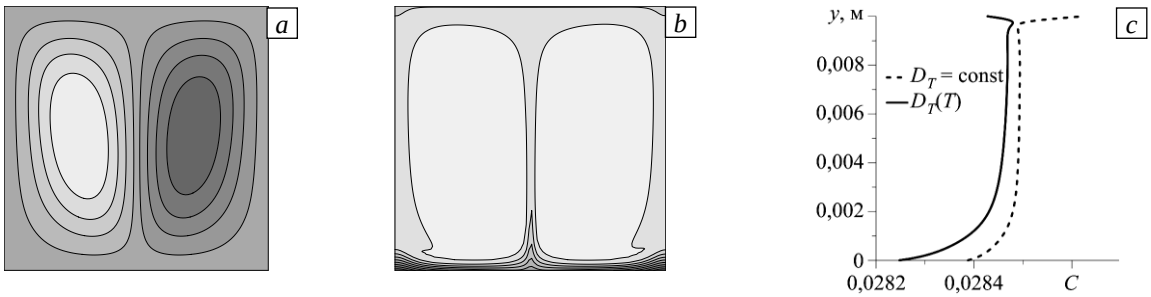

Fig. 6. Isolines of the stream function (*a*), concentration distribution (*b*) at a temperature-dependent thermal diffusion coefficient; concentration profiles (*c*) along the line $x = 0,005$ m at a gravity ten times less than the Earth one, at the time $t = 1000$ s.

In the upper part of the cavity, the influence of the change in the sign of the thermal diffusion coefficient has an impact: the concentration reaches its maximum value at the point where $D_T(T) \approx 0$ m^2/(s·K), to which the concentration gradients are directed (Fig. 6*c*). The maximum concentration value in the case of a constant thermal diffusion coefficient occurs at the upper boundary of the cavity.

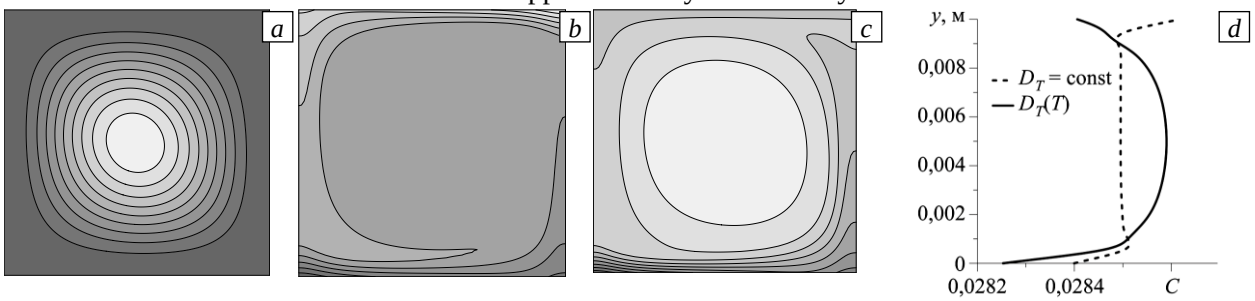

Fig. 8. Isolines of the stream function at a temperature-dependent thermal diffusion coefficient (*a*), the distribution of concentration isolines at a constant (*b*) and variable (*c*) thermal diffusion coefficient; concentration profiles (*d*) along the line $x = 0,005$ m at a gravity one hundred times less than the Earth one, at the time $t = 3600$ s.

3.1.3. The gravitational force is a hundred times less than that of the Earth. With a force of gravity a hundred times less than that of the Earth, a weak stationary flow is realized in a square cavity (Fig. 7*a*), which appears after a sufficiently long non-convective period. The onset of convection is accompanied by an increase in the intensity of movement, which takes place over a time interval from 500 to 850 s. The separation of the mixture in a stationary regime at a constant value of the thermal diffusion coefficient is approximately 1.4 times higher than in case when the dependence $D_T(T)$ is taken into account (Fig. 6*b*).

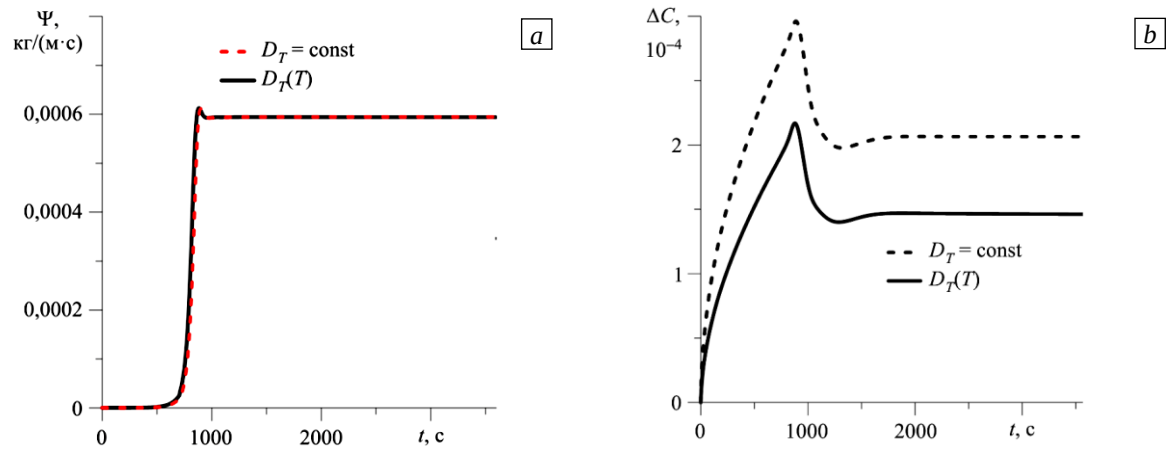

Fig. 7. Temporal evolution of the maximum value of the stream function in the cavity (*a*) and the concentration difference between the centers of the upper and lower boundaries (*b*) at a gravity one hundred times less than the Earth one.

The structure of a stationary flow is one-vortex (Fig. 8) both at a constant thermal diffusion coefficient and at $D_T(T)$. When the temperature dependence is taken into account, the concentration isolines in the flow field are "frozen", as in the previous case (Fig. 8*b*, *c*). The concentration profile along the $x = 0,005$ m line with a variable thermal diffusion coefficient shown in Fig. 8*d* as a solid line differs significantly from the profile obtained with a constant D_T (Fig. 8*d*, dashed line) and is qualitatively similar to the profile in the absence of convection presented in [31].

3.2. Rectangular cavity

3.2.1. Earth gravity. Let us consider the behavior of the mixture in a rectangular cavity with length $l = 0,05$ m and height $h = 0,01$ m. Figure 9 shows the graphs of the temporal evolution of the maximum value of the stream function in the cavity and the concentration difference between the centers of the upper and lower boundaries of the cavity at a constant ($D_T \approx -1,58 \cdot 10^{-12}$ m^2/(s·K)) and variable ($D_T(T)$ (9)) thermal diffusion coefficient.

As can be seen from the figure, taking into account dependence (9) has little effect on the intensity of the flow arising in the cavity. In both situations, there is an almost complete absence of a non-convective period at short times, then a strong flow emerges in the form of irregular oscillations (Fig. 9*a*).

The flow intensity is slightly higher in the case $D_T(T)$, and the separation of the mixture occurs later, and its maximum value is less (Fig. 9*b*).

The flow structure is 4-vortex with a constant and variable coefficient of thermal diffusion, however, in the first case, there are two more vortices, more pronounced than with a temperature-dependent coefficient of thermal diffusion (Fig. 10). Concentration isolines show that in the middle part of the cavity its distribution is uniform, and noticeable changes are observed near the boundaries of the cavity (Fig. 11*a*, *b*). Figure 11*c*, which shows the vertical profiles of the concentration, demonstrates the influence of the change in the sign of the thermal diffusion coefficient, as well as the presence of uniformity in the concentration distribution in the central part of the cavity and its absence at the boundaries.

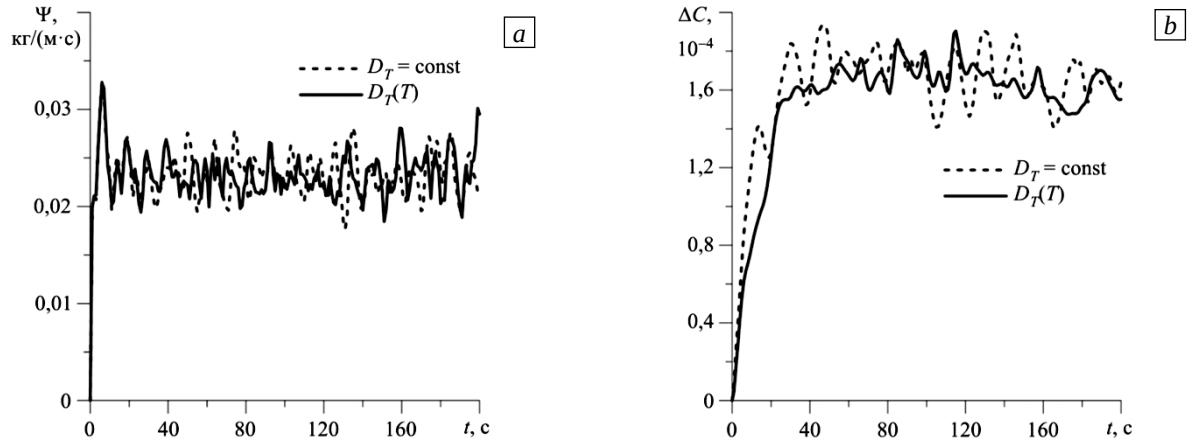

Fig. 9. Temporal evolution of the maximum value of the stream function in the cavity (*a*) and the concentration difference between the centers of the upper and lower boundaries (*b*) under conditions of Earth gravity.

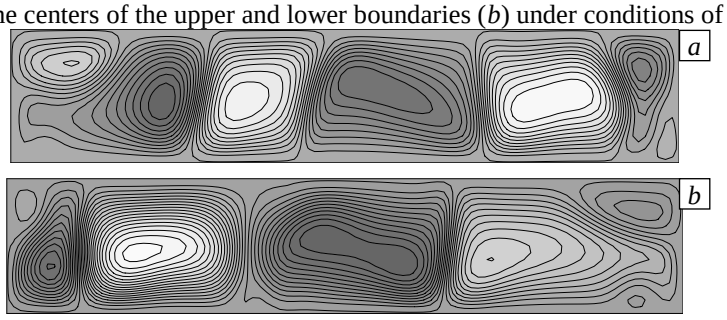

Fig. 10. Isolines of the stream function at a constant (*a*) and temperature-dependent (*b*) coefficient of thermal diffusion under the action of the Earth gravity at time $t = 200$ s.

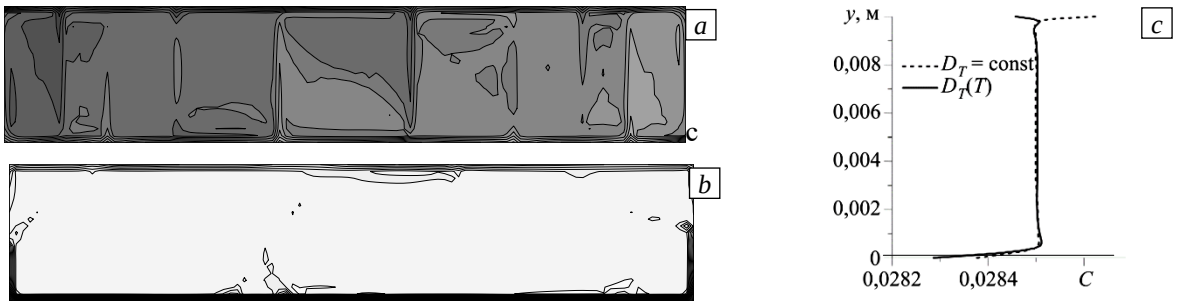

Fig. 11. Distribution of solute concentration at constant (*a*) and temperature-dependent (*b*) thermal diffusion coefficient and concentration profiles (*c*) along the line $x = 0,005$ m at the Earth gravity at time $t = 200$ s.

3.2.2. Gravity that is a ten times less than that of the Earth. In the case when the gravitational force is reduced ten times relative to that of the Earth, a non-convective period appears during $t \approx 20$ s from the beginning of the process (see Fig. 12*a*). During this period, separation of the mixture that is close to purely diffusion takes place (Fig. 12*b*). Then convection occurs, accompanied by a sharp increase in the flow intensity and an even greater increase in the degree of separation of the mixture.

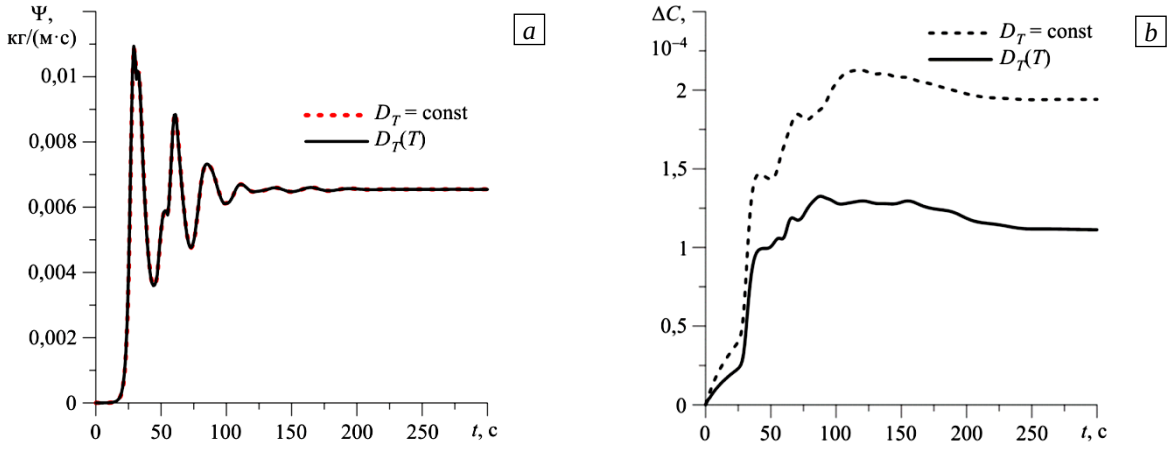

Fig. 12. Temporal evolution of the maximum value of the stream function in the cavity (*a*) and the concentration difference between the centers of the upper and lower boundaries (*b*) at a gravity ten times less than the Earth one.

Then the flow reaches a stationary regime. At the considered value of the gravitational force, the largest values of the difference in the solute concentration in the cavity in the cases of constant and variable coefficients of thermal diffusion differ stronger than under the action of the Earth gravitational force. The differences are even more noticeable compared to the square cavity — approximately 1.8 times (Fig. 12*b*).

The steady flow established under these conditions has a 9-vortex structure at constant D_T and 8-vortex one at a variable $D_T(T)$ (Fig. 13). Compared with the case of the action of the Earth gravity, a decrease in the spatial scale of convective vortices is observed. The Schmidt number is large, because of this, the concentration isolines are "frozen" in the velocity field. Nine regions appear with a constant thermal diffusion coefficient and eight regions with a temperature dependence D_T corresponding to the vortices in Figure 13; in these areas the concentration is practically uniform, and when the thermal diffusion coefficient changes the sign inside the cavity, the “freezing” is more pronounced (Fig. 14*a*, *b*). The concentration profiles show that, as in the case of the Earth gravitational force, the concentration value differs little from the initial value in the central part of the cavity and significantly at the boundaries. However, the difference between the flows of a mixture with constant and variable coefficients of thermal diffusion at a given level of gravity is more noticeable because there is some deviation from the equilibrium value in the central part (Fig. 14*c*). In the case of a flow with a constant thermal diffusion coefficient, in contrast to a flow with a variable $D_T(T)$, the solute concentration is highest at the upper boundary of the cavity.

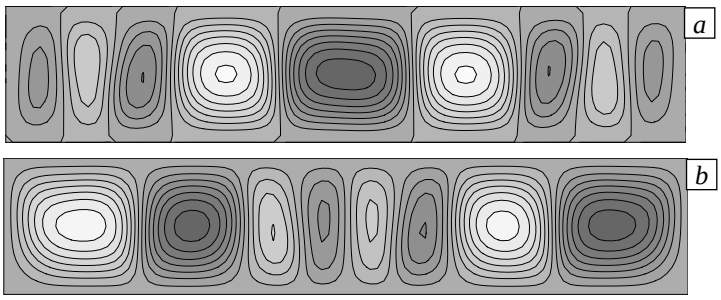

Fig. 13. Isolines of the stream function at a constant (*a*) and temperature-dependent (*b*) coefficient of thermal diffusion at a gravity that is ten times less than the Earth one, at a time $t = 300$ s.

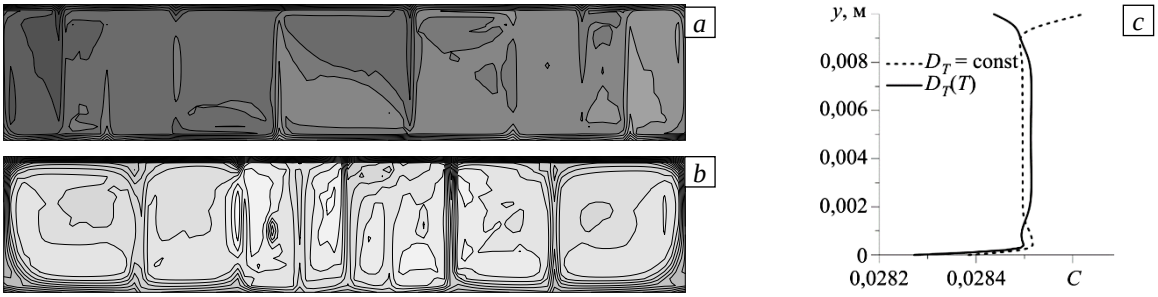

Fig. 14. Distribution of solute concentration at constant (*a*) and temperature-dependent (*b*) coefficient of thermal diffusion and concentration profiles along the line $x = 0,005$ m (*c*) at gravity, ten times less than the Earth one, at time $t = 300$ s.

3.2.3. Gravity that is a hundred times less than that of the Earth. In a field of reduced gravity, a long non-convective period is observed in a rectangular cavity, it continues approximately 250 s (Fig. 15*a*). A further increase in the flow intensity also lasts for a rather long time: the transition to a stationary regime occurs at a time of about 450 s. With a variable coefficient of thermal diffusion, the enhancement of the mixture separation is carried out more slowly than with a constant one (Fig. 15*b*). In this case, the separation of the mixture in a stationary regime decreases 1,6 times as compared with the case of a constant thermal diffusion coefficient.

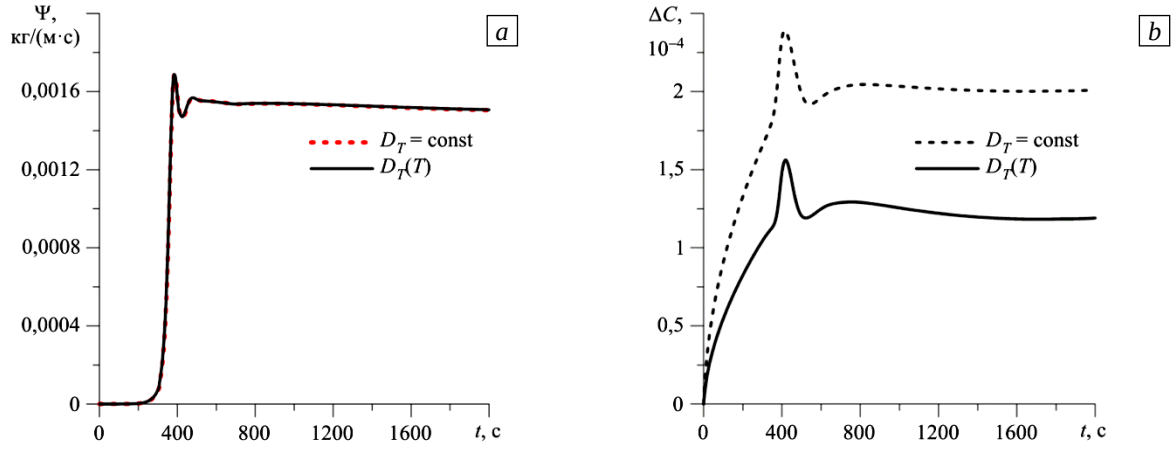

Fig. 15. Temporal evolution of the maximum value of the stream function in the cavity (*a*) and the concentration difference between the centers of the upper and lower boundaries (*b*) at a gravity that is one hundred times less than the Earth one.

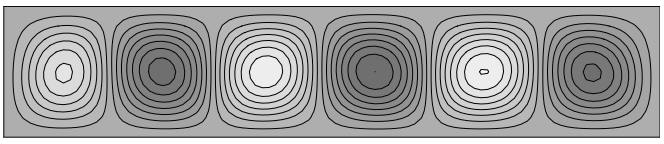

Fig. 16. Isolines of the stream function at a temperature-dependent coefficient of thermal diffusion at a gravity that is one hundred times less than the Earth one, at the time $t = 2000$ s.

The flow structure at $t = 2000$ s, which corresponds to the stationary regime, is shown in Figure 16. It can be seen that the flow has a 6-vortex shape. The concentration isolines, as in the case of a gravity which is 10 times lower, are "frozen" in the stream function field. With a variable coefficient of thermal diffusion, the concentration isolines differ from those obtained in the simulation in the case of a constant coefficient of thermal diffusion; due to change of thermal diffusion coefficient sign, the concentration reaches its maximum value not at the boundary of the cavity, but in its central part (Fig. 17*a*, *b*), therefore, the distribution of the NaCl mixture along the vertical central line in the middle part of the cavity is close to the initial one in Figure 17*a* and differs markedly from the initial one in Figure 17*b*. At the horizontal boundaries, the concentration changes sharply (Fig. 17*c*).

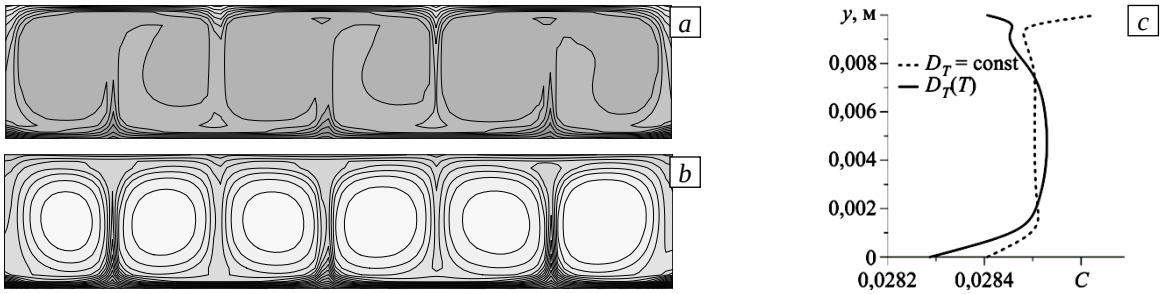

Fig. 17. Distribution of solute concentration at constant (*a*) and temperature-dependent (*b*) coefficient of thermal diffusion and concentration profiles (*c*) along the line $x = 0,005$ m at a gravity that is one hundred times less than the Earth one, at the time $t = 2000$ s.

4. Conclusion

The results of numerical simulation of the onset and development of non-linear regimes of convection of an aqueous NaCl solution in square and rectangular cavities elongated in the horizontal direction are presented. The calculations were performed taking into account the dependence of the thermal diffusion coefficient $D_T(T)$ on temperature according to the polynomial law. Heating from below is considered; the temperature difference between the horizontal boundaries created in this case is 40 K. With such a temperature difference, the mixture inside the cavity changes the sign of the thermal diffusion coefficient, which leads to a change in the direction of the concentration gradient. The emergence and development of convective regimes under conditions of terrestrial and low gravity is investigated. In the case of a square cavity under the Earth gravity, an oscillatory 4-vortex flow with reconnection of vortices is formed. With a decrease in the force of gravity, the flow becomes stationary 2-vortex, and with even less gravity, it becomes single-vortex. In a rectangular cavity under the Earth gravity, irregular fluctuations in the values of the flow characteristics are observed. With a decrease in the gravitational force, the flow becomes stationary, its spatial scale decreases.

The flow intensity is rather high, therefore, a uniform distribution of the mixture is maintained in the central part of the cavity. Large gradients of solute concentration are observed near the boundaries. Taking into account the polynomial dependence of the thermal diffusion coefficient on temperature has little effect on the nature of the flow; however, a change in the sign of the thermal diffusion coefficient inside the cavity leads to a significant decrease, in comparison with the flow of a mixture at a constant thermal diffusion coefficient, of the maximum degree of separation of the components.

This work was carried out with financial support from the government of the Perm Region (Program of Support for Scientific Schools of the Perm Region, Agreement No. C-26/788).

References

1. Galliero G., Bataller H., Croccolo F., Vermorel R., Artola P.-A., Rousseau B., Vesovic V., Bou-Ali M., Ortiz de Zárate J.M., Xu S., Zhang K., Montel F. Impact of thermodiffusion on the initial vertical distribution of species in hydrocarbon reservoirs. *Microgravity Sci. Technol.*, 2016, vol. 28, pp. 79-86. https://doi.org/10.1007/s12217-015-9465-6
2. Maryshev B.S., Lyubimova T.P., Lyubimov D.V. Stability of homogeneous seepage of a liquid mixture through a closed region of the saturated porous medium in the presence of the solute immobilization. *Int. J. Heat Mass Tran.*, 2016, vol. 102, pp. 113-121. https://doi.org/10.1016/j.ijheatmasstransfer.2016.06.016

3. Soboleva E.B. Density-driven convection in an inhomogeneous geothermal reservoir. *Int. J. Heat Mass Tran.*, 2018, vol. 127, pp. 784-798. https://doi.org/10.1016/j.ijheatmasstransfer.2018.08.019
4. Klimenko L.S., Maryshev B.S. Microchannel cleaning by the external laminar flow. *Vestnik Permskogo universiteta. Fizika – Bulletin of Perm University. Physics*, 2020, no. 3, pp. 5-13. https://doi.org/10.17072/1994-3598-2020-3-05-13
5. Lyubimova T.P., Lepikhin A.P., Parshakova Ya.N., Tsiberkin K.B. Numerical modeling of liquid-waste infiltration from storage facilities into surrounding groundwater and surface-water bodies. *J. Appl. Mech. Tech. Phy.*, 2016, vol. 57, pp. 1208-1216. https://doi.org/10.1134/S0021894416070099
6. Sasmito A.P., Birgersson E., Ly H.C., Mujumdar A.S. Some approaches to improve ventilation system in underground coal mines environment – A computational fluid dynamic study. *Tunnelling and Underground Space Technology*, 2013, vol. 34, pp. 82-95. https://doi.org/10.1016/j.tust.2012.09.006
7. Lyubimova T.P., Lepikhin A.P., Parshakova Ya.N. Numerical simulation of wastewater discharge into water objects to improve discharge devices. *Vychisl. mekh. splosh. sred – Computational Continuum Mechanics*, 2019, vol. 12, no. 4, pp. 427-434. https://doi.org/10.7242/1999-6691/2019.12.4.36
8. Lepikhin A.P., Voznyak A.A., Lyubimova T.P., Parshakova Ya.N, Lyakhin Yu.S., Bogomolov A.V. Studying the formation features and the extent of diffuse pollution formed by large industrial complexes: case study of the Solikamsk–Berezniki industrial hub. *Water Resour.*, 2020, vol. 47, pp. 744-750. https://doi.org/10.1134/S0097807820050127
9. Barvier E. Geothermal energy technology and current status: an overview. *Renew. Sustain. Energ. Rev.*, 2002, vol. 6, pp. 3-65. https://doi.org/10.1016/S1364-0321(02)00002-3
10. Kishikawa Y., Shinohara H., Maeda K., Nakamura Y., Wiegand S., Kita R. Temperature dependence of thermal diffusion for aqueous solutions of monosaccharides, oligosaccharides, and polysaccharides. *Phys. Chem. Chem. Phys.*, 2012, vol. 14, pp. 10147-10153. https://doi.org/10.1039/c2cp41183k
11. D'Errico G., Ortona O., Paduano L., Sartorio R. Diffusion properties of the ternary system human serum albumin–sodium cholate–water. *J. Solution Chem.*, 2014, vol. 43, pp. 893-915. https://doi.org/10.1007/s10953-014-0179-y
12. Shliomis M.I., Souhar M. Self-oscillatory convection caused by the Soret effect. *EPL*, 2000, vol. 49, pp. 55-61. http://dx.doi.org/10.1209/epl/i2000-00119-4
13. Cherepanov I.N., Smorodin B.L. Oscillatory convection of a colloidal suspension in a horizontal cell. *Vychisl. mekh. splosh. sred – Computational Continuum Mechanics*, 2020, vol. 13, no. 3, pp. 247-255. https://doi.org/10.7242/1999-6691/2020.13.3.19
14. Demin V.A., Mizev A.I., Petukhov M.I., Shmyrov A.V. Separation of low-melting metal melts in a thin inclined capillary. *Fluid Dyn.*, 2019, vol. 54, pp. 1-13. https://doi.org/10.1134/S001546281901004X
15. Kolodner P., William H., Moe C. Optical measurement of the Soret coefficient of ethanol/water solutions. *J. Chem. Phys.*, 1988, vol. 88, pp. 6512-6524. https://doi.org/10.1063/1.454436
16. Leahy-Dios A., Firoozabadi A. Molecular and thermal diffusion coefficients of alkane-alkane and alkane-aromatic binary mixtures: Effect of shape and size of molecules. *J. Phys. Chem. B*, 2007, vol. 111, pp. 191-198. https://doi.org/10.1021/jp064719q
17. Mialdun A., Shevtsova V.M. Development of optical digital interferometry technique for measurement of thermodiffusion coefficients. *Int. J. Heat Mass Tran.*, 2008, vol. 51, pp. 3164-3178. https://doi.org/10.1016/j.ijheatmasstransfer.2007.08.020
18. Königer A., Meier B., Köhler W. Measurement of the Soret, diffusion, and thermal diffusion coefficients of three binary organic benchmark mixtures and of ethanol/water mixtures using a beam deflection technique. *Phil. Mag.*, 2009, vol. 89, pp. 907-923. https://doi.org/10.1080/14786430902814029
19. Blanco P., Bou-Ali M.M., Platten J.K., de Mezquia D.A., Madariaga J.A., Santamaría C. Thermodiffusion coefficients of binary and ternary hydrocarbon mixtures. *J. Chem. Phys.*, 2010, vol. 132, 114506. https://doi.org/10.1063/1.3354114
20. Vitagliano V., Lyons P.A. Diffusion coefficients for aqueous solutions of sodium chloride and barium chloride. *J. Am. Chem. Soc.*, 1956, vol. 78, pp. 1549-1552. https://doi.org/10.1021/ja01589a011
21. Caldwell D.R. Measurement of negative thermal diffusion coefficients by observing the onset of thermohaline convection. *J. Phys. Chem.*, 1973, vol. 77, pp. 2004-2008. https://doi.org/10.1021/j100635a018
22. Caldwell D.R., Eide S.A. Soret coefficient and isothermal diffusivity of aqueous solutions of five principal salt constituents of seawater. *Deep Sea Res. Oceanogr. Res. Paper.*, 1981, vol. 28, pp. 1605-1618. https://doi.org/10.1016/0198-0149(81)90100-X

23. Chang Y.C., Myerson A.S. The diffusivity of potassium chloride and sodium chloride in concentrated, saturated, and supersaturated aqueous solutions. *AlChE J.*, 1985, vol. 31, pp. 890-894. https://doi.org/10.1002/aic.690310603
24. Mialdun A., Shevtsova V. Temperature dependence of Soret and diffusion coefficients for toluene–cyclohexane mixture measured in convection-free environment. *J. Chem. Phys.*, 2015, vol. 143, 224902. https://doi.org/10.1063/1.4936778
25. Johnson J.-C.C., Beyerlein A.L. Thermal diffusion in mixtures with associated reactions. Thermal diffusion factors for methanol-benzene mixtures. *J. Phys. Chem.*, 1978, vol. 82, pp. 1430-1436. https://doi.org/10.1021/j100501a021
26. Wittko G., Kohler W. On the temperature dependence of thermal diffusion of liquid mixtures. *EPL*, 2007, vol. 78, 46007. https://doi.org/10.1209/0295-5075/78/46007
27. Zhang K.J., Briggs M.E., Gammon R.W., Sengers J.V. Optical measurement of the Soret coefficient and the diffusion coefficient of liquid mixtures. *J. Chem. Phys.*, 1996, vol. 104, pp. 6881-6892. https://doi.org/10.1063/1.471355
28. Ghorayeb K., Firoozabadi A. Modeling multicomponent diffusion and convection in porous media. *SPE J.*, 2000, vol. 5, pp. 158-171. https://doi.org/10.2118/62168-PA
29. Shevtsova V.M., Melnikov D.E., Legros J.C. Onset of convection in Soret-driven instability. *Phys. Rev. E*, 2006, vol. 73, 047302. https://doi.org/10.1103/PhysRevE.73.047302
30. Lyubimova T., Zubova N., Shevtsova V. Effects of non-uniform temperature of the walls on the Soret experiment. *Microgravity Sci. Technol.*, 2019, vol. 31, pp. 1-11. https://doi.org/10.1007/s12217-018-9666-x
31. Ryzhkov I.I., Stepanova I.V. On thermal diffusion separation in binary mixtures with variable transport coefficients. *Int. J. Heat Mass Tran.*, 2015, vol. 86, pp. 268-276. https://doi.org/10.1016/j.ijheatmasstransfer.2015.02.069
32. Weast R.C. (Ed.) *Handbook of chemistry and physics*. CRC Press, 1977.
33. Cooper C.A., Glass R.J., Tyler S.W. Effect of buoyancy ratio on the development of double-diffusive finger convection in a Hele-Shaw cell. *Water Resour. Res.*, 2001, vol. 37, pp. 2323-2332. https://doi.org/10.1029/2001WR000343
34. Gershuni G.Z., Zhukhovitskii E.M. *Convective stability of incompressible fluids*. Keter Publishing House, 1976. 330 pp.
35. Lyubimova T., Rushinskaya K., Zubova N. Onset and nonlinear regimes of convection of a binary mixture in rectangular cavity heated from below. *Microgravity Sci. Technol.*, 2020, vol. 32, pp. 961-972. https://doi.org/10.1007/s12217-020-09823-x

The authors declare no conflict of interests.
The paper was received on 22.03.2021.
The paper was accepted for publication on 09.06.2021.